

Synthesizing reconfigurable foot traces using a Klann mechanism

Jaichandar Kulandaidasan Sheba^{†,‡,*}, Mohan Rajesh Elara[§], Edgar Martínez-García[‡] and Le Tan-Phuc[†]

[†]*School of Electrical and Electronics Engineering, Singapore Polytechnic, Singapore*

[‡]*Institute of Engineering and Technology, Universidad Autónoma de Ciudad Juárez, Mexico*

[§]*Engineering Product Development Pillar, Singapore University of Technological Design, Singapore*

(Accepted January 28, 2015. First published online: March 2, 2015)

SUMMARY

Legged locomotion systems have been effective in numerous robotic missions, and such locomotion is especially useful for providing better mobility over irregular landscapes. However, locomotion capabilities of robots are often constrained by a limited range of gaits and the associated energy efficiency. This paper presents the design of a novel reconfigurable Klann mechanism capable of producing a variety of useful gait cycles. Such an approach opens up new research avenues, opportunities and applications. The position analysis problem that arises when dealing with reconfigurable Klann mechanisms was solved here using a bilateration method, which is a distance-based formulation. By changing the linkage configurations, our aim was to generate a set of useful gaits for a legged robotic platform. In this study, five gait patterns of interest were identified, analysed and discussed that validate the feasibility of our approach and considerably extend the capabilities of the original design.

KEYWORDS: Klann mechanism; Reconfigurable linkage; Legged robot; Foot trajectory; Bilateration.

1. Introduction

In recent years, research and development of legged robots have gained significant momentum from the worldwide robotics research community, reflected by the grandeur of initiatives at universities, companies and governments. Most legged robot designs are inspired from and mimic the structures and functions of natural systems.^{1,2} Such legged robots often have the ability to move through irregular, abrupt terrains and exhibit significantly improved versatility and manoeuvrability compared to wheeled robots, which can only move on prepared land. Compared to wheeled or robots on tracks, legged robots have the potential to transverse certain types of terrain in a more efficient and stable manner.³ For legged robots, contact with the ground is discontinuous, which enables them to select footholds for avoiding obstacles and therefore cause less damage to their surroundings when manoeuvring in cluttered and tight environments. However, any direct realization of natural locomotion methods in an artificial legged robot is highly challenging due to the complexity of the mechanical structure, the many degrees of freedom required of one leg for smooth movement, complicated control algorithms and energy consumption issues. Typically, each leg of a legged robot is designed using three to six actuators to control the movement of each leg. This helps the leg move flexibly and produces numerous gaits. However, the use of many actuators requires a more complex controller and more energy to drive. Therefore, the development of a mechanism that can meet the requirements for both flexible movement and low energy consumption using a simple control algorithm is essential. The traditional method used to achieve different gaits is to add more actuators. By utilizing a reconfigurable Klann mechanism, we are able to generate different gaits suitable for a

* Corresponding author. E-mail: jai@sp.edu.sg

given task without changing the number of actuators, thereby reducing the controller complexity and the energy required to drive the actuators.

In nature, not all legged species have the same locomotion. For example, mammals, reptiles and insects have different walking gaits and can only utilize a limited number of gaits constrained by their species' morphology. Similarly, a robot that has a fixed structure and movement mechanism faces challenges related to the constrained set of gaits that it can produce. Numerous research efforts have been dedicated to solving this limitation by developing various design strategies. One such design concept is the interconnection of many small, simple and fewer degree of freedom robots to create a new, more functional structure.^{4–6} However, such an approach results in increasing difficulty in the control algorithms when many units are connected together. Another reported design approach achieves gait variations via parametric changes of the leg structure.^{7–10} Nansai *et al.*¹¹ introduced a novel method in which a robot adjusts its hardware morphology by modifying the length ratio of its legs to produce many gaits with only one degree of freedom, based on the Theo Jansen mechanism. Based on such a parametric design approach, our aim in this study is to design a robot using a Klann mechanism that can change its linkage configurations to adapt its gait according to changes in the surrounding environment.

For legged robots, there are many different approaches for generating gait patterns, including adaptive locomotion control,^{12,13} the combination of rigid and tensile structural elements,¹⁴ morphological computation,¹⁵ the use of an oscillator controller with pneumatic actuators⁷ and biomimetic adaptations based on ground contact timing¹⁶ or sensorimotor coordination.¹⁷ Previous studies have not applied a Klann-based reconfigurable design, and the novelty of the presented work lies in the application of the technique using a Klann mechanism. Here, a Klann-based reconfigurable design is presented in which a robot changes its structural morphology by modifying its components and sub-assembly parameters to adapt to multi-terrains and multi-tasks.

Our approach can be used to design an energy efficient system that reduces the computation load on the controller. The leg linkage length ratio of the robot platform has been modified to create a large pool of gait patterns, which can be selectively used by the robots to explore and test its surroundings, to acquire real feedback, and to learn new transformation approaches that will enable its locomotion capability at any given time. This reconfigurable mechanism approach can be extended from a symmetrical two-legged assembly to a four- or more-legged assembly. The design of a reconfigurable robot based on a single Klann mechanism is presented in this paper. This design supports multi-legged robots that incorporate adaptive changes when one leg fails and the ability to use a leg as a tool to perform functions other than locomotion. This design can be applied to both homogenous- and heterogeneous-legged platforms. The developed design can be used in surveillance applications for traversing various terrains while utilizing less energy and in rescue missions that require manoeuvring over uneven terrain with limited power.

The rest of the paper is organized as follows: Section 2 introduces the Klann linkage used in this study and the distance-based formulation using a bilateration method to identify the position of the robot's foot. Section 3 recognizes some sample gaits generated from a simulation of the reconfigurable design. Section 4 presents a transforming procedure for the reconfigurable leg between two different gaits. In Section 5, a preliminary CAD design of the reconfigurable Klann linkage is provided, and Section 8 gives a conclusion of this study along with a discussion of future work.

2. Single Klann Linkage

The Klann linkage (also referred to as the “Klann leg” in this paper), named after its inventor, is a planar mechanism that is formed by six bars connected to one another by revolute joints. This linkage was designed to transfer the rotating motion of a crank into movement of a foot, similar to the gait of legged animals. The design incorporates the ability to cross uneven terrain while providing a smooth, even ride using only one actuator. The Klann mechanism is an extension of Burmester curves that translates the rotary motion of a crank shaft to the linear motion of a foot for one-half of a rotation and elevation the foot for the other half of the rotation, thus returning the crank to its original position. Two of these linkages placed 180° out of phase serve as a substitute for a wheel. The limitation of this mechanism is that it can produce only one walking gait for one specific design of linkages. The foot trajectory of the standard Klann planar mechanism is designed to simulate the gait of a legged animal.^{18–22} The main challenge in identifying foot trajectory for further reconfigurable designs is

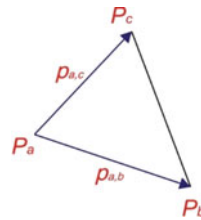


Fig. 1. The bilateration problem.

to create efficient approaches to solve the position analysis problem of the Klann leg. A common method is to solve a system of nonlinear equation with the number of equations equal to the number of unknown variables.²³ However, the elimination process yields a large number of solutions caused by trigonometric parts and tangent half-angle problems. For this type of problem, Rojas²⁴ introduced an alternative method based on bilateration that does not rely on variable eliminations or trigonometric substitutions, which is clarified in the following section.

2.1. Kinematics of a Klann linkage: bilateration

The bilateration problem consists of finding feasible locations of a point, say P_c , given its distances to two other points, say P_a and P_b , whose locations are known. Then, according to Fig. 1, the solution to this problem can be expressed in matrix form as:

$$p_{a,c} = Z_{a,b,c} p_{a,b}, \tag{1}$$

Where $p_{a,b} = \overrightarrow{P_a P_b}$, and $Z_{a,b,c} = \frac{1}{2s_{a,b}} \begin{bmatrix} s_{a,b} + s_{a,c} - s_{b,c} & -4A_{a,b,c} \\ 4A_{a,b,c} & s_{a,b} + s_{a,c} - s_{b,c} \end{bmatrix}$, is called a bilateration matrix, with $s_{a,b} = d_{a,b}^2 = P_{a,b}^2$, the squared distance between P_a and P_b , and $A_{a,b,c} = \pm \frac{1}{4} \sqrt{(s_{a,b} + s_{a,c} + s_{b,c})^2 - 2(s_{a,b}^2 + s_{a,c}^2 + s_{b,c}^2)}$.

The oriented area of $\Delta P_a P_b P_c$ is defined as positive if P_c is to the left of vector $p_{a,b}$, and vice versa. Interested readers can refer to ref. [25] for a detailed analysis of the equation presented. Using bilateration matrices, the position analysis problem of linkages, such as a Klann leg, is greatly simplified. Next, we apply the bilateration method to a Klann leg for solving the position analysis problem of the foot.

2.2. Klann linkage: system of equations

Figure 2 shows a Klann leg with five links: $\overline{P_1 P_2}$, $\overline{P_3 P_4}$, $\overline{P_5 P_6}$, $\overline{P_2 P_3 P_7}$ and $\overline{P_6 P_7 P_8}$. This one degree-of-freedom planar linkage consists of the frame ($\Delta P_1 P_4 P_5$), one crank (segment $\overline{P_1 P_2}$), two grounded rockers (segments $\overline{P_3 P_4}$, $\overline{P_5 P_6}$), and two couplers ($\Delta P_2 P_3 P_7$, $\Delta P_6 P_7 P_8$) all connected by revolute joints. These links and the dimensions of the frame, including the link lengths $d_{1,2}$, $d_{2,3}$, $d_{3,4}$, $d_{5,6}$, $d_{3,7}$, $d_{6,7}$ and $d_{7,8}$, and the fixed angles ε and ω of the two couplers, and an input angle θ are all known. The Cartesian coordinate plane O_{xy} includes the original point placed on joint P_1 together with axis directions, as shown. The position analysis problem for the Klann leg then calculates all of the possible Cartesian locations of the end point P_8 .

In this case, squared distances and the bilateration matrix are used to compute the corresponding location of the end point P_8 based on angle θ . First, let us locate the position of P_3 by computing $p_{2,3}$ from θ and the positions of joints P_2 and P_4 using Eq. (1):

$$p_{2,3} = Z_{2,3,4} p_{2,4} \tag{2}$$

$$\Leftrightarrow \overrightarrow{P_2 P_3} = \frac{1}{2s_{2,4}} \begin{bmatrix} s_{2,4} + s_{2,3} - s_{4,3} & -4A_{2,4,3} \\ 4A_{2,4,3} & s_{2,4} + s_{2,3} - s_{4,3} \end{bmatrix} \overrightarrow{P_2 P_4}.$$

With $\overrightarrow{P_2 P_4} = \overrightarrow{P_4} - \overrightarrow{P_2} = \begin{pmatrix} x_4 - d_{1,2} \cos \theta \\ y_4 - d_{1,2} \sin \theta \end{pmatrix}$, $A_{2,4,3} = \frac{1}{4} \sqrt{(s_{2,4} + s_{2,3} + s_{4,3})^2 - 2(s_{2,4}^2 + s_{2,3}^2 + s_{4,3}^2)}$

(P_3 is to the left of vector $\overrightarrow{P_2 P_4}$ in this case), and $s_{2,4} = \overrightarrow{P_2 P_4}^2 = (x_4 - d_{1,2} \cos \theta)^2 +$

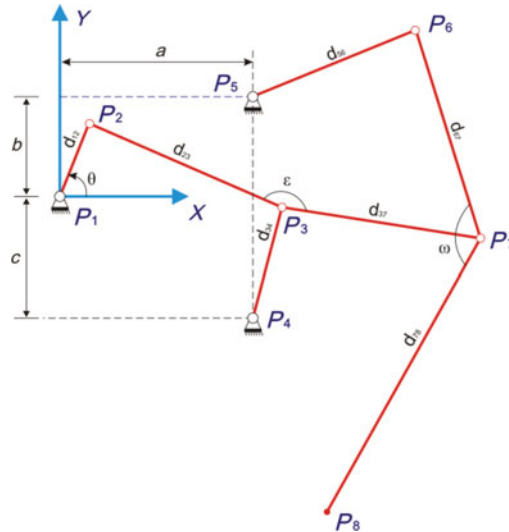


Fig. 2. Klann linkage.

$$(y_4 - d_{1,2} \sin \theta)^2.$$

After obtaining, we can calculate $\vec{P}_3 = \vec{P}_2\vec{P}_3 + \vec{P}_2$. (3)

Next, we locate P_7 based on P_2 and P_3

$$p_{2,7} = Z_{2,3,7} p_{2,3},$$

$$\Leftrightarrow \vec{P}_2\vec{P}_7 = \frac{1}{2s_{2,3}} \begin{bmatrix} s_{2,3} + s_{2,7} - s_{3,7} & -4A_{2,3,7} \\ 4A_{2,3,7} & s_{2,3} + s_{2,7} - s_{3,7} \end{bmatrix} \vec{P}_2\vec{P}_3.$$
(4)

With $s_{2,7} = s_{3,2} + s_{3,7} - 2d_{3,2}d_{3,7} \cos(\epsilon)$, $A_{2,3,7} = \frac{1}{4}\sqrt{(s_{2,3} + s_{2,7} + s_{3,7})^2 - 2(s_{2,3}^2 + s_{2,7}^2 + s_{3,7}^2)}$ (P_7 is to the left of vector $\vec{P}_2\vec{P}_3$ in this case).

$$\vec{P}_7 = \vec{P}_2\vec{P}_7 + \vec{P}_2.$$
(5)

Then, from P_7 and P_5 , P_6 is located

$$p_{5,6} = Z_{5,7,6} p_{5,7},$$
(6)

$$\Leftrightarrow \vec{P}_5\vec{P}_6 = \frac{1}{2s_{5,7}} \begin{bmatrix} s_{5,7} + s_{5,6} - s_{7,6} & -4A_{5,7,6} \\ 4A_{5,7,6} & s_{5,7} + s_{5,6} - s_{7,6} \end{bmatrix} \vec{P}_5\vec{P}_7.$$

With $s_{5,7} = \vec{P}_5\vec{P}_7^2$, $A_{5,7,6} = \frac{1}{4}\sqrt{(s_{5,7} + s_{5,6} + s_{7,6})^2 - 2(s_{5,7}^2 + s_{5,6}^2 + s_{7,6}^2)}$ (P_6 is to the left of vector $\vec{P}_5\vec{P}_7$ in this case).

$$\vec{P}_6 = \vec{P}_5\vec{P}_6 + \vec{P}_5.$$
(7)

Continuing this process, we locate point P_8 from P_6 and P_7 . We have the following:

$$p_{6,8} = Z_{6,7,8} p_{6,7},$$
(8)

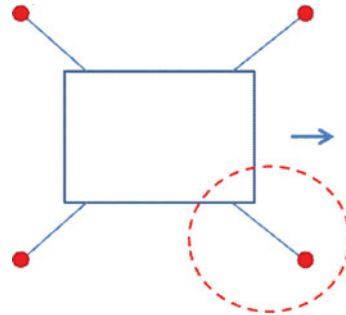


Fig. 3. The right-front leg was chosen for the analyses in this paper.

$$\Leftrightarrow \overrightarrow{P_6P_8} = \frac{1}{2s_{6,7}} \begin{bmatrix} s_{6,7} + s_{6,8} - s_{7,8} & -4A_{6,7,8} \\ 4A_{6,7,8} & s_{6,7} + s_{6,8} - s_{7,8} \end{bmatrix} \overrightarrow{P_6P_7}.$$

With $s_{6,8} = s_{7,6} + s_{7,8} - 2d_{7,6}d_{7,8} \cos(\omega)$, $A_{6,7,8} = -\frac{1}{4}\sqrt{(s_{6,7} + s_{6,8} + s_{7,8})^2 - 2(s_{6,7}^2 + s_{6,8}^2 + s_{7,8}^2)}$ (P_8 is to the right of vector $\overrightarrow{P_6P_7}$ in this case).

$$\rightarrow \overrightarrow{P_8} = \overrightarrow{P_6P_8} + \overrightarrow{P_6}. \tag{9}$$

From Eqs. (5) and (7), the positions of points P_7 and P_6 , respectively, are located. Equation (9) defines the position of point P_8 , the foot of the Klann leg, which depends on the set of link dimensions (S), including the fixed angles ω and ε , the input angle (θ), the locations of P_1 , P_4 and P_5 , and the oriented areas $A_{2,4,3}$, $A_{2,3,7}$, $A_{5,7,6}$ and $A_{6,7,8}$. Instead of using independent loop-closure equations with joint angles, for a specific set of link dimensions (S) and angle θ of the Klann leg, a unique position of the end point P_8 is located using the bilateration method described above.

3. Identification of Foot Traces of the Klann Leg for Intra-Reconfigurability

3.1. Standard Klann leg foot trajectory

Our study aims to identify novel, useful gait patterns for the reconfigurable Klann leg that satisfy one or more of the following objectives: gait imitation of different animal species; improvements in the locomotion efficiency for a range of ground conditions; and transformations of mechanisms into tools for different purposes such as manipulation, digging, etc. To achieve these goals, we first must identify the foot trajectory of a standard Klann leg. This foot trajectory will be used for further analyses, comparisons and evaluations of the new reconfigurable foot traces presented in this paper. As this study represents an initial step for the design of a complete reconfigurable platform using Klann linkages, we chose one leg at the front-right side for the analysis presented here, as shown in Fig. 3. Hereafter, all link dimensions and simulation results relating to foot trajectories in this paper are associated with this leg.

We select $s_{1,2} = 110^2$, $s_{2,3} = 280^2$, $s_{3,4} = 130^2$, $s_{3,7} = 230^2$, $s_{5,6} = 170^2$, $s_{6,7} = 260^2$, $s_{7,8} = 490^2$, $\varepsilon = 170^0$ and $\omega = 160^0$ as the standard dimensions for the Klann leg and three points of frame, $P_1 = (0, 0)^T$, $P_4 = (260, -130)^T$, $P_5 = (260, 60)^T$ shown in Fig. 4. Using these dimensions, we compute the position of every point P_8 using the series of equations presented in Section 2 with input θ value. By connecting all of the calculated points, we trace the gait pattern following these steps:

1. Evaluate the sign of all of the oriented areas $A_{2,4,3}$, $A_{2,3,7}$, $A_{5,7,6}$ and $A_{6,7,8}$ of the current leg.
2. Compute the location of P_8 using Eqs. (2)–(9).
3. Increase the value of θ at a specific rate, providing a full crank rotation from 0 to $2\pi rad$ to collect all of the feasible points of P_8 .



Fig. 4. Standard dimensions of a Klann leg (Left). A 3D model for a quadruped robot using Klann linkages (Right).

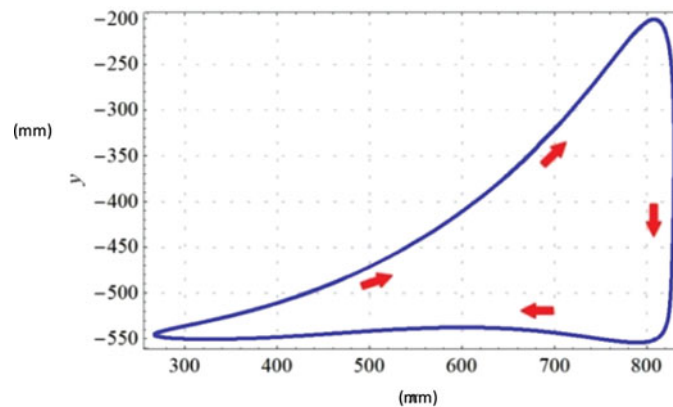


Fig. 5. Traced foot trajectory of a standard Klann leg where the trajectory direction corresponds to counter-clockwise rotation of the crank.

4. Connect all of the feasible points, and present the points on Fig. 5. The red arrows indicate the direction of the foot trajectory, which in this case corresponds to counter-clockwise rotation of the crank.

For a standard Klann leg, the foot trajectory used on walking platforms can be easily traced based on the geometric structure of the Klann linkage in Fig. 4, where the signs of the oriented areas should follow $A_{2,3,4} > 0$, $A_{2,3,7} > 0$, $A_{5,6,7} > 0$ and $A_{6,7,8} < 0$. Interestingly, the standard foot trajectory of a Klann leg is quite similar to that of spiders during single step cycles.

With a different set of link dimensions, we can acquire a distinct foot trajectory for each set. Hence, if the Klann leg could change the link dimensions itself, the linkage will generate numerous new and different coupler curves. Under this basic principle, our objective in this study is to identify whether small variations in the lengths of the links of a standard Klann leg can yield novel foot trajectories of interest for a walking platform. Hence, a simple exploratory method is conducted in which we change the standard dimensions of every link of the Klann leg within $\pm 25\%$, except the crank ($d_{1,2}$), the leg ($d_{7,8}$) and the frame (P_1, P_4, P_5). Then, all of the resulting foot coupler curves are computed using the above method for each change in the link dimensions. Useful, potential gait patterns are selected manually from the coupler curve results for further innovative applications. By applying this idea, we discovered various patterns of interest, which are briefly described in the following part. We restricted the overall range to be within certain values for better operation and stability, considering the constraints of real world environments. The Link dimensions before and after transformation and Linear actuator travelling limits are given in Table II and Table III respectively.

3.2. Classification of different gait patterns of the reconfigurable design

3.2.1. Digitigrade locomotion. The standard foot trajectory of a Klann leg is similar to the long stride of spider locomotion. However, digitigrades walk on their digits or toes. Animals that use this type of locomotion include dogs, cats, many other mammals, and most birds.²⁶ Due to the short floor touch of the foot of digitigrades, these animals induce less friction while walking and therefore use less

energy. This feature makes digitigrade locomotion of great interest for the development of walking platforms.²⁷

In Table I, the first row labelled “4 links” shows the foot trajectory of a Klann leg when the length dimensions of the links P_3P_7 , P_5P_6 , P_6P_7 and ε are decreased by 17%, increased by 12%, decreased by 15% and increased by 10^0 . With these changes in the configuration of link lengths, the Klann leg switches its gait from that of a spider to a digitigrade. Columns “5 links” and “6 links” in the first row of Table I present other modifications of the link dimensions that further illustrate digitigrade behaviours. The foot trajectory is plotted below the corresponding configuration. For each Figure, the gait of the standard Klann leg is presented as a blue-dashed curve, and the reconfigurable curve is shown in red colour. These conventions are applied for all of the following cases.

3.2.2. Jam avoidance (walking on soft, sticky terrain). When walking on soft or sticky terrain, such as semi-wet mud, walkers may easily become jammed due to the soil conditions. Usually, the walker’s gait pattern must be altered such that their strides become shorter, and the touch-down and lift-up leg angles are increased nearly to 90° to overcome such situations. Figure 5 shows that standard trajectory of the Klann leg has a high contact angle of nearly 90° but a very low lift angle, which leads to energy inefficiency of the walking cycle and a tendency to become stuck.

A gait with the potential to solve this issue is presented in the second row, column “4 links” of Table I. Such a curve is obtained increasing the distances of P_2P_3 , P_3P_4 , P_3P_7 and P_5P_6 by 7%, 23%, 9% and 12%, respectively. In addition to a higher walking pattern, this trajectory provides a higher lift angle with a shortened stride compared to the standard Klann leg trajectory. Other combinations of link dimensions of the Klann leg for jam avoidance trajectories are depicted in the second row, columns “5 links” and “6 links” of Table I.

3.2.3. Step climbing. One of the advantages of a standard Klann leg is that it has a high foot step at 350 (units), with highest point at -200 (units), which can handle uneven terrain or insignificant obstacles, such as gravel or small stones. However, the difficulty is increased when the leg is faced with higher step levels (above -200 units) or obstacles of greater height than its limit (350 units).

The third row of Table I shows adjustments in the link dimensions of a standard Klann leg that generate foot trajectories for climbing steps. This curve results from increasing the distance of P_3P_4 by 15% and P_3P_7 by 9% and decreasing the distance of P_2P_3 by 4% and P_5P_6 by 12%, which is provided in column “4 links”. In this case, the height of the foot trajectory is approximately 500 (units), which is 42.85% higher than the normal trajectory. Columns “5 links” and “6 links” indicate other link modifications for which the step height is significantly increased and the foot can reach over the horizontal line of the x -axis.

3.2.4. Hammering motion. In addition to the walking-related foot patterns presented above, in the process of analysing foot trajectories for a reconfigurable design, we identified a potential pattern whose shape is similar to a hammering motion. The hammering action provides repeated, short, rapid impacts to an object with high force on a small area. The fourth row of Table I presents a configuration of the link dimensions of a standard Klann leg that provides a foot trajectory simulating hammering motion. The curve in first column can be obtained by increasing the distances of P_2P_3 by 18%, P_3P_4 by 15%, and P_6P_7 by 15% and by decreasing the distance of P_3P_7 by 9%. With this reconfigurable characteristic, we go one step beyond a simple walking Klann linkage. By changing the link dimensions of a standard leg, we not only modify the gait patterns of the walking platform for the purpose of walking, but also can change the behaviour of the system for performing other tasks.

3.2.5. Digging motion. In many legged animals such as dogs or cats, legs are used not strictly for walking or running but also for other functions, such as pawing, clawing or digging, etc. These movements can be useful in various situations; for example, the digging motion is especially useful during exploration. Therefore, we consider the ability of a robot to dig and to break the solid ground for exploring and collecting soil samples in dangerous environments as highly important. The last row of Table I shows that a reconfigurable Klann leg can create such a digging trajectory for applications related to exploration and security missions. The leg can produce a digging cycle with the minimum changes in link dimensions shown in column “4 links,” where the distances of P_2P_3 , P_5P_6 and P_6P_7 are increased by 7%, 12% and 8%, respectively, and P_3P_7 is reduced by 17%. This type of motion is

Table I. Identified foot trajectory patterns of interest for reconfiguration applications.

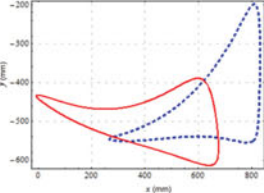
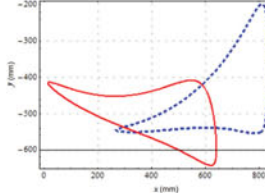
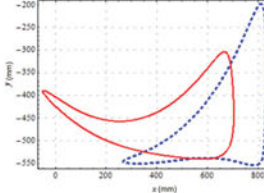
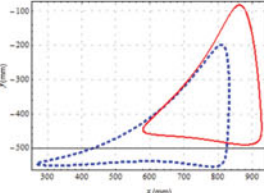
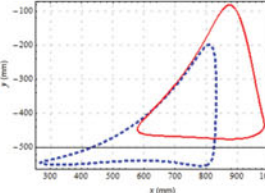
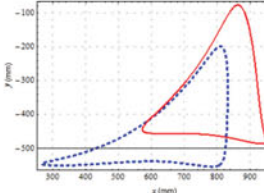
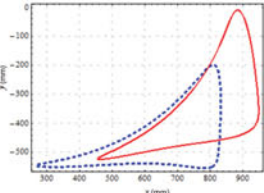
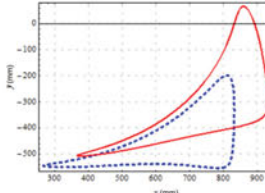
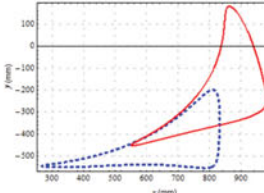
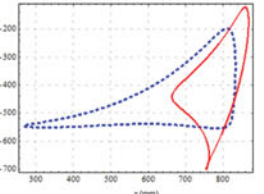
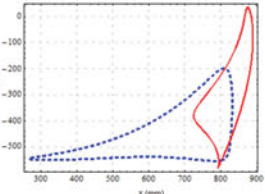
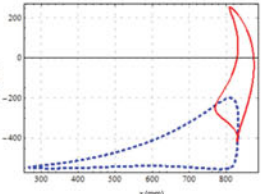
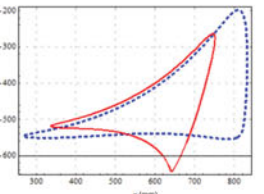
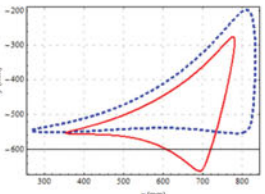
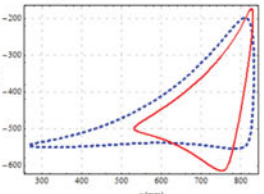
Patterns	4 links	5 links	6 links
Digitigrade locomotion	$d_{3,7} : -17\%$, $d_{5,6} : +12\%$, $d_{6,7} : -15\%$, $\varepsilon : +10^0$ 	$d_{2,3} : +4\%$, $d_{3,7} : -17\%$, $d_{5,6} : +15\%$, $d_{6,7} : -23\%$, $\varepsilon : +10^0$ 	$d_{2,3} : -7\%$, $d_{3,4} : +15\%$, $d_{3,7} : -17\%$, $d_{5,6} : +12\%$, $d_{6,7} : -15\%$, $\varepsilon : +10^0$ 
Jam avoidance	$d_{2,3} : +7\%$, $d_{3,4} : +23\%$, $d_{3,7} : +9\%$, $d_{5,6} : +12\%$ 	$d_{2,3} : +7\%$, $d_{3,4} : +23\%$, $d_{3,7} : +17\%$, $d_{5,6} : +17\%$, $d_{6,7} : -4\%$ 	$d_{2,3} : +7\%$, $d_{3,4} : +8\%$, $d_{3,7} : +17\%$, $d_{5,6} : +18\%$, $d_{6,7} : -4\%$, $\varepsilon : -10^0$ 
Step climbing	$d_{2,3} : -4\%$, $d_{3,4} : +15\%$, $d_{3,7} : +9\%$, $d_{5,6} : -12\%$ 	$d_{2,3} : -7\%$, $d_{3,4} : +15\%$, $d_{3,7} : +9\%$, $d_{6,7} : -15\%$, $\varepsilon : -10^0$ 	$d_{2,3} : -7\%$, $d_{3,4} : +23\%$, $d_{3,7} : +17\%$, $d_{5,6} : -12\%$, $d_{6,7} : -8\%$, $\varepsilon : -10^0$ 
Hammering motion	$d_{2,3} : +18\%$, $d_{3,4} : +15\%$, $d_{3,7} : -9\%$, $d_{6,7} : +15\%$ 	$d_{2,3} : +14\%$, $d_{3,4} : +15\%$, $d_{3,7} : -9\%$, $d_{6,7} : +15\%$, $\varepsilon : -10^0$ 	$d_{2,3} : +7\%$, $d_{3,4} : +15\%$, $d_{3,7} : -9\%$, $d_{5,6} : +6\%$, $d_{6,7} : +4\%$, $\varepsilon : -30^0$ 
Digging motion	$d_{2,3} : +7\%$, $d_{3,7} : -17\%$, $d_{5,6} : +12\%$, $d_{6,7} : +8\%$ 	$d_{2,3} : +7\%$, $d_{3,7} : -17\%$, $d_{5,6} : +12\%$, $d_{6,7} : +8\%$, $\varepsilon : +10^0$ 	$d_{2,3} : +11\%$, $d_{3,4} : +15\%$, $d_{3,7} : -17\%$, $d_{5,6} : -12\%$, $d_{6,7} : +8\%$, $\varepsilon : +10^0$ 

Table II. Link dimensions before and after transformation.

Link dimension	l_A (mm)	l_B (mm)
$d_{3,4}$	160	130
$d_{3,7}$	250	190
$d_{6,7}$	260	290

Table III. Linear actuator travelling limits.

Actuator	Min length	Max length
$d_{2,3}$	260	330
$d_{4,3}$	130	160
$d_{3,7}$	190	270
$d_{5,6}$	150	200
$d_{6,7}$	200	280
ε	140°	180°

quite similar to the hammering motion. However, the leg is pulled back after contacting the ground, instead of lifting up the foot, immediately after reaching the lowest point.

4. Characterization of Leg Transformation

In the previous section, we assessed a variety of gait patterns of interest for reconfigurable robotic applications together with their link configurations of a Klann leg. The next challenge for the design process of a reconfigurable Klann regards how the leg can properly transform among gait patterns without any problems, such as

1. The leg performing a transformation between two gaits while its leg is up over the ground. This can cause the entire platform to become unbalanced if the leg is attached to the robot.
2. A free transformation without control may also lead to undesired floor contact if the foot goes below ground level and unexpectedly harms the linkage.

To prevent the above problems, we propose a simple procedure for transforming a reconfigurable Klann leg between two patterns, pattern A and pattern B, in which both A and B belong to the set of patterns mentioned in Section 3 (standard locomotion, digitigrade locomotion, jam avoidance, digging motion, hammering motion or step climbing). We review the transformation from jam avoidance locomotion ($d_{2,3} : +7\%$, $d_{3,4} : +23\%$, $d_{3,7} : +9\%$, $d_{5,6} : +12\%$) to digging motion ($d_{2,3} : +7\%$, $d_{3,7} : -17\%$, $d_{5,6} : +12\%$, $d_{6,7} : +8\%$) as a proof of concept. The transformation method is accomplished through 12 steps, as follows:

1. For jam avoidance (pattern A), from the current position of the frame, including three revolute joints P_1 , P_4 and P_5 , define the lowest value of $P_{8,y}$ with the corresponding input angle θ , say θ_A , using the set of equations in Section 2, increasing θ at a specified rate. For this transformation example of jam avoidance locomotion to digging locomotion, for $P_1 = (0, 0)^T$, $P_4 = (260, -130)^T$, $P_5 = (260, 30)^T$, and increments of 0.01 rad for θ , we obtain $\theta_A = 0.37$ rad (Fig. 6 (right-top)).
2. Repeat step 1 for digging motion (pattern B). In our example, we obtain $\theta_B = 6.09$ rad (Fig. 6 (right-top)).
3. Specify the transformation time values for the entire process. The transformation initializes at time $t = t_1$ and finalizes at time $t = t_2$. The transformation time can be defined as $\Delta t = t_2 - t_1$. For the example here, we choose $\Delta t = 3$ with $t_1 = 0.5$ and $t_2 = 3.5$ (Fig. 6 (right-bottom)). This Δt value is chosen within a suitable range to ensure that the leg transformation does not occur too slowly while also not affected by inertial force, which can make the platform unbalanced.
4. From patterns A and B, identify the link dimensions that must be modified from an l_A value at time $t = t_1$ (pattern A) to an l_B value at time $t = t_2$ (pattern B). In our example, the links are:

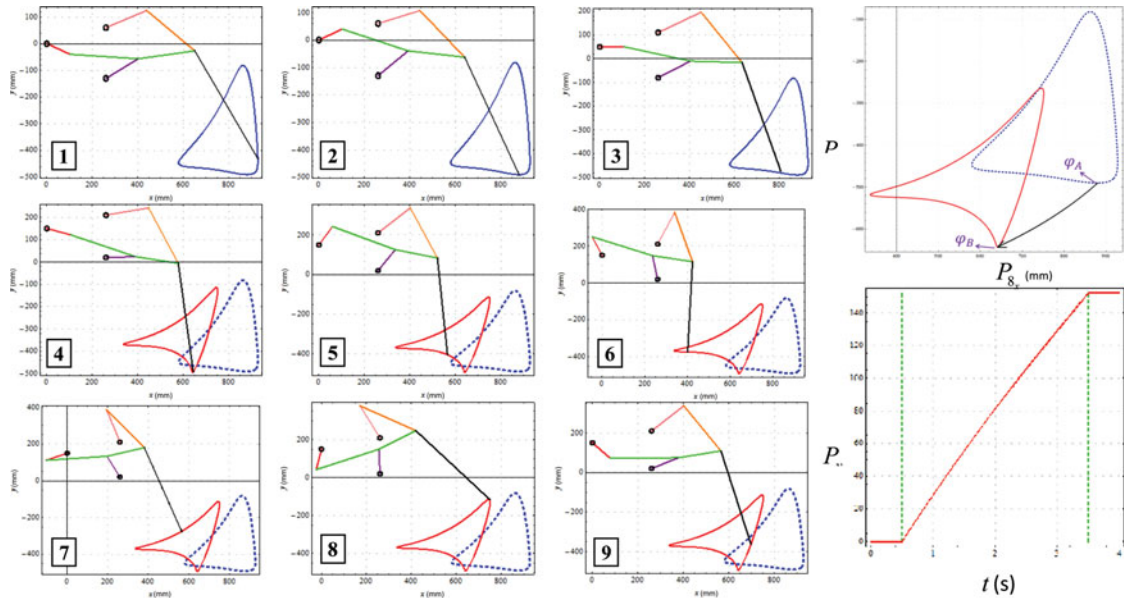


Fig. 6. Transformation from jam avoidance locomotion ($d_{2,3} : +7\%$, $d_{3,4} : +23\%$, $d_{3,7} : +9\%$, $d_{5,6} : +12\%$) to digging motion ($d_{2,3} : +7\%$, $d_{3,7} : -17\%$, $d_{5,6} : +12\%$, $d_{6,7} : +8\%$). **Left:** Several steps of the leg transformation are simulated. The links that change in dimension during the transformation process are highlighted in purple ($d_{3,4}$), light green ($d_{3,7}$) and orange ($d_{6,7}$). The foot trajectories before and after the transformation are also illustrated, where jam avoidance locomotion is shown in dotted blue and digging motion is shown in red. **Right-top:** The lowest points of P_8 in the y -axis for each of the trajectories of the conversion are linked by a black arrow. This arrow also indicates the movement of the foot when transforming between two trajectories. The initial and final input angles, θ_A and θ_B , are also determined in the transformation process. **Right-bottom:** The changing progress of P_y (the entire linkage) from $t = t_1$ to $t = t_2$.

5. Start the transformation, setting $t = t_1$. Bring the foot to the transformation point by increasing the input angle from the current θ to $\theta = \theta_A$ (computed in step 1), and define the location of the foot, say P_{8c} .
6. For each link dimensions listed in step 4, compute $l_i = \frac{l_B - l_A}{\Delta t} (t - t_1)$, where l_i is the increment length of the corresponding link at specific time t . Then, the new link length, defined as $l_n = l_A + l_i$, can be calculated.
7. Now, calculate $\theta_i = \frac{\theta_B - \theta_A}{\Delta t} (t - t_1)$, where θ_i is the increment value of the input angle, and new input angle is $\theta_n = \theta_A + \theta_i$.
8. After obtaining the new dimensions of each variable links l_n , angle θ_n together with the fixed link dimensions and the current locations of the frame with the three revolute joint centres P_1 , P_4 and P_5 , compute the new foot location, say P_{8n} , using Eqs. (2)–(9).
9. Compute the offset $\Delta y = P_{8n_y} - P_{8c_y}$ and set $P_{8c} = P_{8n}$.
10. Define $P_y = P_c - \Delta y$ as the compensate value for any height difference that occurs during the transformation process between the two trajectories, where P_c is the current position of the frame (P_1 , P_4 , P_5). Update the vertical position of the frame to the new value P_y . The evolution of P_y from $t = t_1$ to $t = t_2$ is described in Fig. 6 (right-bottom). This step ensures that the Klann leg will not make any undesired floor contact or loose balance of the entire linkage.
11. Increase time t at a specified rate δt , that is, $t = t + \delta t$. In our example, $\delta t = 0.01(s)$.
12. Repeat steps 6 to 10 until $t = t_2$.

Figure 6 (left) shows a simulation of the leg transformation from jam avoidance ($d_{23} : +7\%$, $d_{34} : +23\%$, $d_{37} : +9\%$, $d_{56} : +12\%$) to digging motion ($d_{23} : +7\%$, $d_{37} : -17\%$, $d_{56} : +12\%$, $d_{76} : +8\%$) through several steps. Notice the vertical change of the frame (P_1, P_4, P_5) from steps 2 to 4 (Fig. 6 (left)) that compensates for the height difference. The leg reaches the lowest position of pattern A (jam avoidance) at step 2 (Fig. 6) and begins to transform. The conversion finishes at step 4, and the entire walking cycle continues corresponding to the digging motion (pattern B). After the transformation

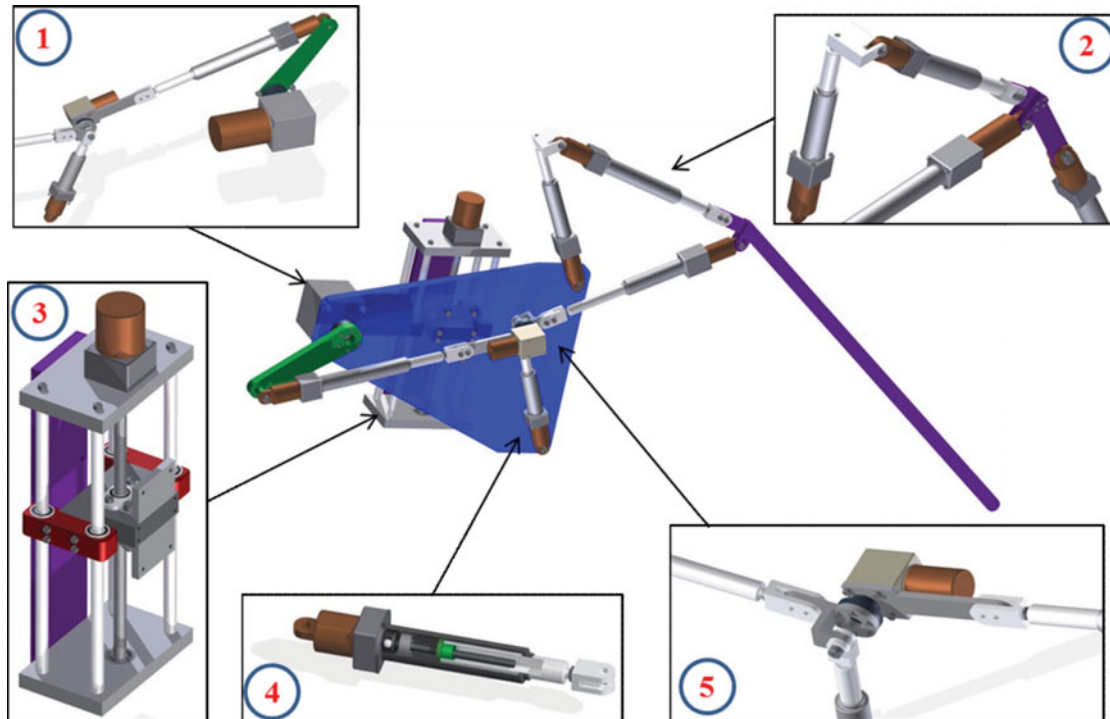


Fig. 7. A fully-functional reconfigurable Klann leg design (centre) with seven actuators suitable for the transformation procedure presented in Section 4.

process is complete, the height of the trajectory can be adjusted as suitable for the final purpose (digging, hammering, etc.).

5. Cad Design of Reconfigurable Klann Leg

After describing novel, useful patterns of a reconfigurable Klann leg in Section 3 and completing the transformation method between two patterns in Section 4, we propose a CAD design of a reconfigurable Klann leg using six linear actuators, one angular actuator and one main motor to drive the linkage, as shown in Fig. 7. The linear actuators act as switches from one trajectory to another trajectory. Following the results of Table I, where a maximum of six dimensions are changed, the six actuators are used to replace the links $d_{2,3}$, $d_{4,3}$, $d_{3,7}$, $d_{5,6}$, $d_{6,7}$ and ε . One vertical linear actuator (Fig. 7 (number 3)) is ***used for height compensation, which was introduced in step 10 of Section 4. The zoomed areas of Fig. 7, denoted 1, 2 and 5, present the construction details of the variable links and the crank driven by the main motor. A potential linear actuator design is also proposed (Fig. 7 (number 4)) that uses ball screws to translate rotational motion to linear motion with little friction and high precision. Based on the standard linkage dimensions, which were introduced in Section 3, and the simulation results given in Table I, the linear actuators are designed with the selected travelling capabilities, as follows:

As shown in Table I, the lowest foot point for the jam avoidance motion, given in column “5 links,” is higher than the lowest point of all other motions, corresponding to -475 (unit). Conversely, the lowest foot point for the hammering motion, given in column “4 links,” is lower than the lowest foot point of all other motions, corresponding to -699 (unit). Hence, for the vertical linear actuator, the travelling distance is limited to 225 (unit) to ensure that it can compensate for all transformations made between any two trajectories given in Table I.

6. Implementation of a Reconfigurable Klann Leg

A fully functional reconfigurable Klan leg was designed using five actuators suitable for performing the transformations discussed in Section 4. The transformations are achieved by changing the link

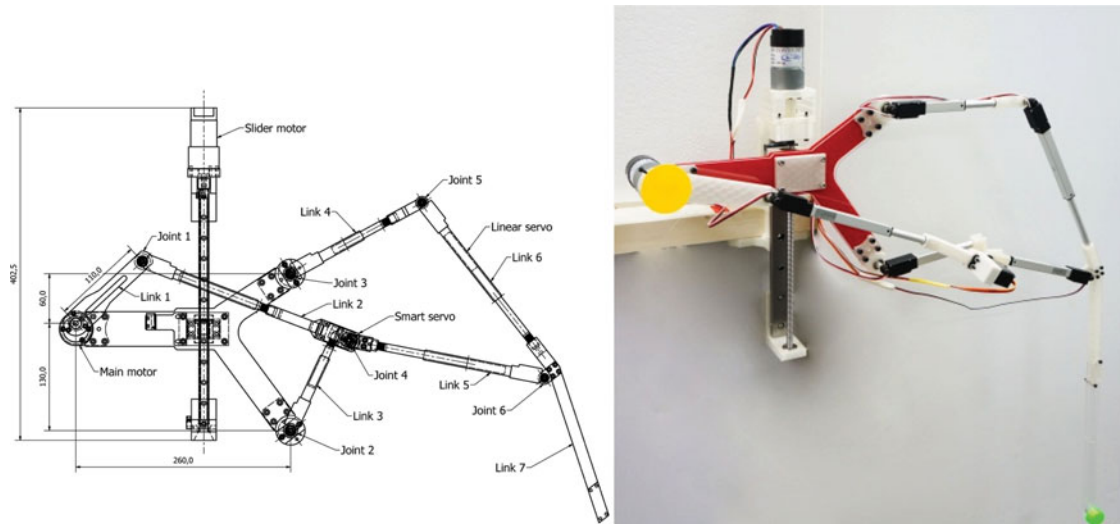


Fig. 8. Detailed design of the reconfigurable Klann linkage.

length variables, as per Table I. To facilitate up-and-down movement during the reconfigurable process, the base link is designed with a ball screw and a slider joint. The base link is designed to allow the up-and-down movement of the reconfigurable Klann leg during the transformation process. The base system and the extendable links are the principal components of the proposed design of the reconfigurable Klann leg. Figure 8 shows a working prototype. The parts needed for the links are fabricated using a 3D printer.

6.1. Klann mechanical design

6.1.1. Links, joints and frame design. After validating the preliminary design using Autodesk Inventor, we modified the linear actuator and slider design based on real parts available on the market to develop a final design for prototyping. The proposed design of the reconfigurable Klann linkage includes two part groups: the leg and the slider. The reconfigurable leg has 7 links, where 5 of the links (link 2, link 3, link 4, link 5 and link 6 shown in Fig. 8) are changeable-length links and the remaining 2 links (link 1 and link 7) are fix-length links. Double ball bearings are used to improve the accuracy of joints 1 to 6. A limit switch is positioned at the point where the crank reaches its horizontal position to define the home position of the crank. Every part of the linkage was designed based on real dimensions, assembled, and simulated using Autodesk Inventor. After all simulations were performed to validate any conflict among the parts of the linkage, we fabricated a prototype of the linkage using a 3D printer for further testing and to obtain real results.

6.1.2. Slider design for height compensation. Figure 9 shows the detailed design of the slider, which includes two main parts: a lead screw and a slide rail. This slider is responsible for compensating for the height difference between two trajectories when the leg performs a transformation to avoid undesired contact with the ground. The dimensions of the slide rail, the lead screw, and other parts are presented in Fig. 9 (right). As the maximum height change can be up to 250 mm between two trajectories, the lead screw and the slide rail are chosen to have sufficient length to account for a 250 mm difference. One limit switch is placed at the bottom, defining the home position. The upper limit is calculated inside the control program based on the slider motor's encoder resolution and the pitch of the lead screw. The lead screw and the slider motor shaft coaxial are critical for providing smooth rotation throughout the range of motion.

6.1.3. Servo motors specifications. To control the speed and position of the crank and the slider, two DC servo motors are used in this design: one is responsible for leg movement and another is responsible for the leg's height. These motors are selected to have the minimum tolerance at the output shaft to ensure precision while being controlled by a close-loop PID controller. The main motor shaft is connected to the crank (link 1), and the slider motor shaft is connected to the lead

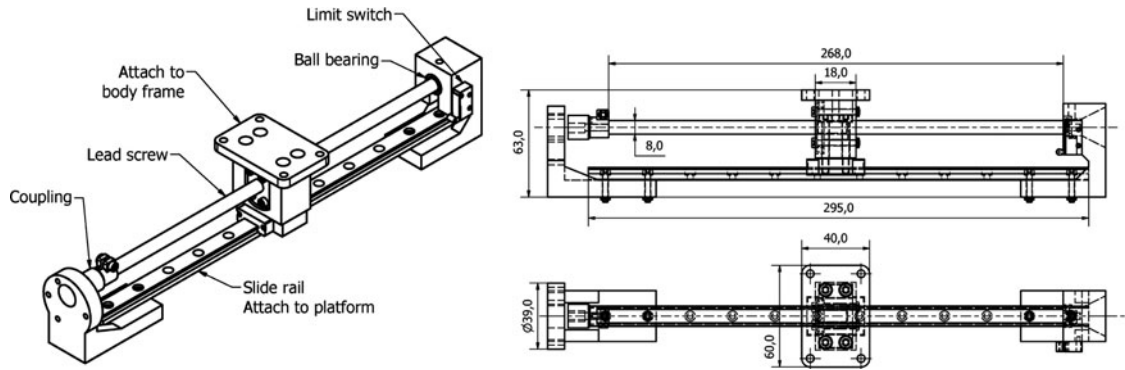


Fig. 9. Details of the slider design.

Table IV. Motor specifications.

Motor specification	Crank	Slider
Gearbox ratio	1:200	1:20
Rotational speed	17 rpm	185 rpm
Torque	784 mNm	78 mNm
Encoder resolution	2400 ppr	240 ppr
Encoder type	Incremental – A,B	
Dimension (D*L)	36*60 mm	

Table V. Motor specifications.

Stroke option	50 mm	100 mm
Positional accuracy	0.2 mm	0.3 mm
Max side force (fully extended)	30 N	15 N
Max speed	12 mm/s	
Peak efficiency	12 N @ 8 mm/s	

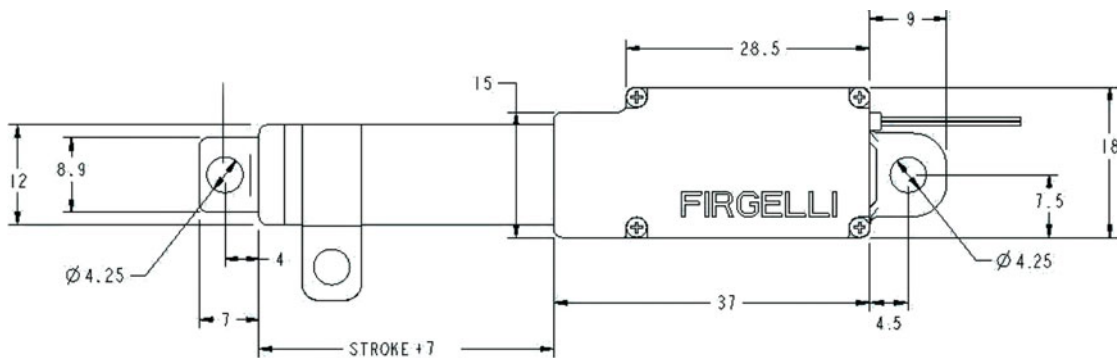


Fig. 10. Dimensions of the Firgelli L12 series linear servo.

screw, as shown in Fig. 8. Due to the speed requirement for the input angle and vertical change of the slider, the motors are chosen according to the specifications listed in Table IV.

The changeable-length links, including link 2, link 3, link 4, link 5 and link 6, can be divided into two groups based on the maximum change in length of their changing ranges: 50 mm or 100 mm. We selected Firgelli L12 series linear servos, shown in Fig. 10, with strokes of 50 mm and 100 mm for the two groups of links. This kind of linear servo provides a variety of lengths, sufficient stroke, and a compact design that allows it to fit in every link of the design. In addition, it requires only one PWM signal to control the stroke length. The specifications of the linear servo are presented in Table V.

Table VI. Motor specifications.

DRS-0101 specification	Max value
Input voltage	7.4 V
Speed	0.166s/600 @ 7.4 V
Torque	12 kgf.cm @ 7.4 V
Angle limit	3200

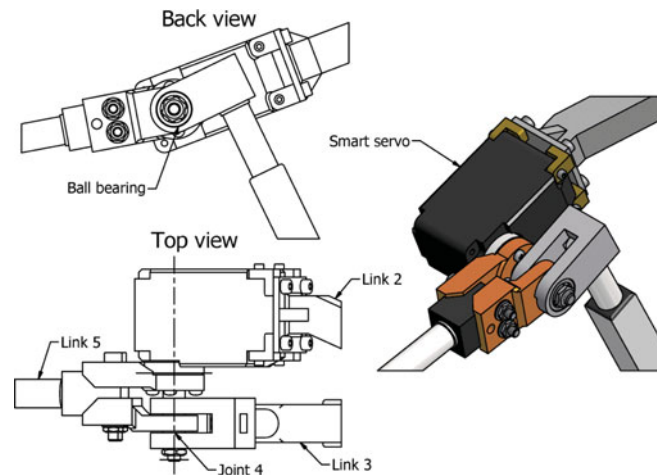


Fig. 11. Detailed design of joint 4 including the smart servo.

To change the angle of joint 4 between links 2 and 5, which allows for the transformation of the leg among different configurations, a Herkulex DRS-0101 smart servo is used at joint 4, as shown in Fig. 11. This smart servo provides high holding torque, high precision with closed-loop control algorithm, and a serial interface with individual IDs for multipoint communication. In particular, in the design of joint 4 (Fig. 11), links 2 and 5 maintain the aspect angle while rotating within a limit corresponding to link 3 at the same time. In addition, the double ball bearing design at joint 4 and at other joints also helps to reduce the error caused by imprecise fabrication of parts. The specifications of the servo are presented in Table VI.

7. Experimental Results and Validation

Testing was conducted to assess the effectiveness of the design and the prototype of the reconfigurable Klann leg for generating several gait patterns and performing transformations. In the experiments, the crank and the compensation slider are driven by 12 V motors with 600 ppr and 60 ppr encoders, respectively, at a constant speed with the PI controller ($P = 17$, $I = 0.1$, sample time $t = 10$ ms). The Firgelli linear servos were used as links $d_{2,3}$, $d_{3,7}$, $d_{3,4}$, $d_{5,6}$, $d_{6,7}$ of the reconfigurable Klann leg. An STM32F0-Discovery board was used as a control CPU to handle all input signals from the two encoders of the DC servos and the output signal for controlling the two DC servos and the five linear servos. The gait trajectories of the prototype were then recorded and processed on a computer using OpenCV library to retrieve the curve and coordinates of the trajectories. The obtained experimental results are discussed below.

7.1. Generation of gait patterns

The first experiment compared the simulated and experimental leg trajectories among different gait patterns. The linear servo link dimensions of the reconfigurable Klann leg were set according to the combinations of parameters given in column “4 links” of Table I together with five cycles of the input crank. The results of this procedure are shown in Fig. 12 for the six gait patterns: standard locomotion, digitigrade locomotion, jam avoidance, step climbing, hammering motion and digging motion. Table VII shows the error and error percentage when comparing the width and the height of the

Table VII. Numerical analysis of the experimental results.

Pattern		Simulation (mm)	Experiment (mm)	Error (mm)	Error percentage (%)	Standard deviation (mm)
Standard locomotion	Height	355.7	392.3	36.6	10.3	3.58
	Width	565.3	625.5	60.1	10.6	4.15
Digitigrade locomotion	Height	223.7	244.6	20.8	9.3	2.78
	Width	684.0	689.7	5.7	0.8	4.30
Jam avoidance	Height	408.5	436.2	27.6	6.8	3.70
	Width	347.9	393.9	46.0	13.2	3.85
Step climbing	Height	515.1	559.6	44.4	8.6	3.88
	Width	492.3	525.3	32.9	6.8	3.68
Hammering motion	Height	577.4	626.7	49.2	8.5	4.05
	Width	204.6	215.6	11.0	5.3	2.97
Digging motion	Height	378.6	411.8	33.2	8.8	3.60
	Width	413.7	402.8	10.9	2.6	3.46

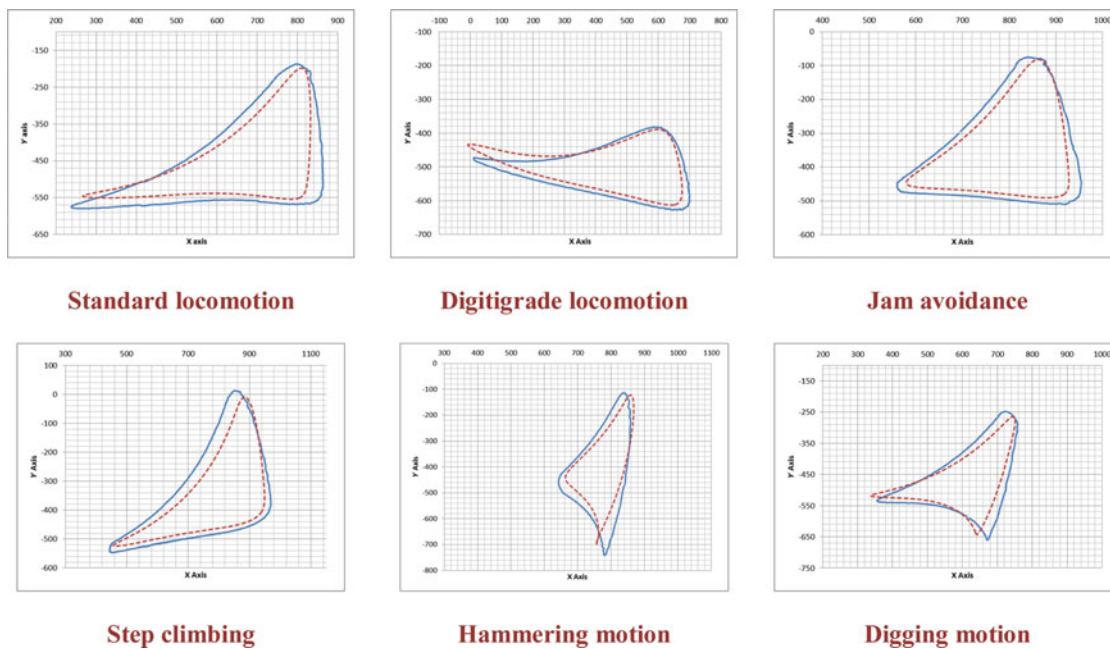


Fig. 12. Comparison of different gait trajectories between experimental trajectories (blue curves) and simulated trajectories (red-dot curves). All of the experimental leg trajectories correspond to data collected from five cycles of the input joint and calculating their median value.

average experimental trajectories with those of the simulated trajectory. For each of the gait patterns presented in Fig. 12, a percent error of less than 13.2% was obtained for all cases. The origin of these errors is primarily due to the non-conformity of link lengths and the presence of joint clearances in the prototype. Both error sources are nearly always inherent to the fabrication of mechanical designs and are the typical elements that affect the performance of linkages and mechanisms.²⁰ The highest error of the digging motion pattern, 8.8% in height, is caused by the dramatic change in the moment generated by the mechanism. It can be shown by simulation that the farthest centre of mass point, with respect to the base link, is achieved for this pattern, and as a consequence, the joint clearance (backlash effect) affects this pattern more than the others. Table VII also presents the standard deviation of the experimental leg trajectories for each of the evaluated patterns. For all of the cases, the standard deviation is small, illustrating the good repeatability of the developed prototype.

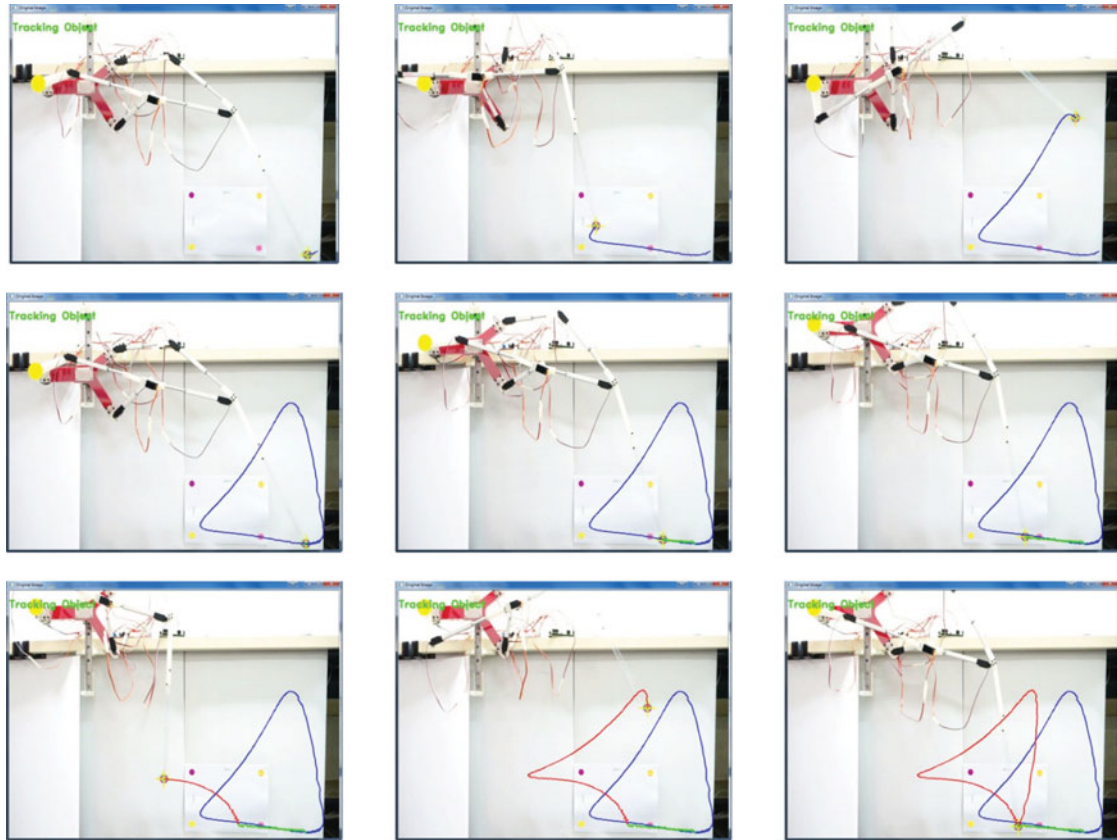


Fig. 13. Experimental results of the transformation process (green curve) from jam avoidance locomotion (blue curve) to digging motion (red curve). Nine captured images from a video analysis program depicting the entire transformation process.

7.2. Leg transformation

The second experiment verified the transformation process presented in Section 4. The transformation from jam avoidance locomotion to digging motion was tested. In this experiment, the start time of the transformation was set to $t_0 = 5$ s with a transformation time of $\Delta t = 180$ s. Figure 13 shows nine snapshots of the experiment, highlighting the corresponding leg trajectories during the process. The results verify that the transformation is carried out without undesired floor contacts.

8. Conclusion

In this paper, we have presented an original reconfigurable design of a legged robot, which we designed using Klann linkages. This design, which is able to transform its links to produce five different gait patterns, is still considered as a one degree-of-freedom linkage when operating in its normal cycle. Seven actuators, which were implemented in the linkage to adjust the link parameters, allow the linkage to produce novel and useful gait trajectories that can be used for many applications in addition to walking. A simple but effective method to solve the position analysis problem for Klann linkages based on a bilateration matrix method and a leg transformation technique were introduced. Five potential gait patterns of the reconfigurable design were classified and evaluated, in addition to a transformation method to allow for switching among the gaits. These typical gait patterns show that this simple yet original Klann linkage can produce foot trajectories not only for walking, but also as tools for performing other functions. Finally, a preliminary CAD design and a single leg prototype, which includes actuators for reconfigurable functions, were presented along with implementation and experimental results. A real Klann leg based on this preliminary design was assembled to test the output trajectories. Furthermore, to evaluate the precision and effectiveness of the linkage, data of real foot traces were collected and compared to simulation results, as presented in Table I. Our long-term

goal is to finalize a complete step-by-step platform with four or more legs to test locomotion, the ability for reconfiguration, and stability, etc. on various types of terrain.

References

1. R. E. Mohan, W. S. Wijesoma, C. A. A. Calderon and C. Zhou, "Experimenting false alarm demand for human robot interactions in humanoid soccer robots," *Int. J. Soc. Robot.* **1**(2), 171–180 (2009).
2. X. Chen, L.-Wang, X. Ye, G. Wang and H. Wang, "Prototype development and gait planning of biologically inspired multi-legged crablike robot," *Mechatronics* **23**, 429–444 (2013).
3. A. Ghassaei, The Design and Optimization of a Crank-Based Leg Mechanism *Ph.D. Thesis* (Claremont, CA: Pomona College Department of Physics and Astronomy, 2011).
4. B. Piranda, G. J. Laurent, J. Bourgeois, C. Clévy, S. Möbes and N. L. Fort-Piat, "A new concept of planar self-reconfigurable modular robot for conveying microparts," *Mechatronics* **23**, 906–915 (2013).
5. H. Y. K. Lau, A.W.Y. Ko and T. L. Lau, "The design of a representation and analysis method for modular self-reconfigurable robots," *Robot. Comput.-Integr. Manuf.* **24**, 258–269 (2008).
6. P. Moubarak and P. Ben-Tzvi, "Modular and reconfigurable mobile robotics," *Robot. Auton. Syst.* **60**, 1648–1663 (2012).
7. K. Tsujita, T. Kobayashi, T. Inoura and T. Masuda, "Gait Transition by Tuning Muscle Tones using Pneumatic Actuators in Quadruped Locomotion," *Proceedings of the IEEE/RSJ International Conference on Intelligent Robots and Systems (IROS)*, France (2008) pp. 2453–2458.
8. F. I. Sheikh and R. Pfeifer, "Adaptive locomotion on varying ground conditions via a reconfigurable leg length hopper," *Adapt. Mobile Robot.* **23**, 527–535 (2012).
9. A. Alamdari, R. Héryn and V. N. Krovi, "Quantitative Kinematic Performance Comparison of Reconfigurable Leg-Wheeled Vehicles," *Proceedings of the 16th International Conference on Climbing and Walking Robots Australia CLAWAR*, (2013).
10. J. E. Pratt and B. T. Krupp, "Series Elastic Actuators Legged Robots," *Proceedings of the SPIE*, Florida USA (2004) pp. 135–144.
11. S. Nansai, N. Rojas, M. R. Elara and R. Sosa, "Exploration of Adaptive Gait Patterns with a Reconfigurable Linkage Mechanism," *Proceedings of the IEEE/RSJ International Conference on Intelligent Robots and Systems (IROS)*, Japan (2013) pp. 4661–4668.
12. A. Kamimura, H. Kurokawa, E. Yoshida, S. Murata, K. Tomita and S. Kokaji, "Automatic locomotion design and experiments for a modular robotic system," *IEEE/ASME Trans. Mechatronics* **10**(3), 314–325 (2005).
13. S. Ha, Y. Han and H. Hahn, "Adaptive Gait Pattern Generation of Biped Robot based on Human's Gait Pattern Analysis," *Proceedings of the 23rd World Academy of Science, Engineering and Technology*, (2007) pp. 80–85.
14. C. Paul, J. W. Roberts, H. Lipson and F. V. Cuevas, "Gait Production in a Tensegrity Based Robot," *Proceedings of the 12th International Conference on Advanced Robotics*, (2005) pp. 216–222.
15. C. Paul, "Morphological computation: A basis for the analysis of morphology," *Robot. Auton. Syst.* **54**(8), 619–630 (2006).
16. J. G. Cham, J. K. Karpick and M. R. Cutkosky, "Stride period adaptation for a biomimetic running hexapod," *Int. J. Robot. Res.* **23**(2), 141–153 (2004).
17. Y. Fukuoka, H. Kimura and A. H. Cohen, "Adaptive dynamic walking of a quadruped robot on irregular terrain based on biological concepts," *Int. J. Robot. Res.* **22**, 187–202 (2003).
18. J. C. Klann, "Walking Device," *U.S. Patent* No. 6,478,314. (12 Nov. 2002).
19. J. C. Klann, "Walking Device," *U.S. Patent* No. 6,260,862. (17 Jul. 2001).
20. R. D. Allen, "Multi-Legged, Walking Toy Robot," *U.S. Patent* No. 5,423,708. (13 Jun. 1995).
21. N. G. Lokhande and V. B. Emche, "Mechanical Spider by Using Klann Mechanism," *IJMCA* **1.5** (2013) pp. 013–016.
22. T. Shannon, Development of a Museum-Quality Display of Mechanisms, *Diss. Massachusetts Institute of Technology*, (2011).
23. B. V. Gilho and J. M. Bezerra, "Mechatronic Design of a Chair for Disabled with Locomotion by Legs," *ABCM Symposium Series in Mechatronics* vol. 5, (2012), pp. 1142–1149.
24. N. Rojas and F. Thomas, "On closed-form solutions to the position analysis of Baranov trusses," *Mech. Mach. Theory* **50**, 179–196 (2012).
25. N. Rojas, "Distance-based formulations for the position analysis of kinematic chains," (2012).
26. E. Muybridge, *Animals in motion* (Courier Dover Publications, 2012) USA.
27. S. M. Reilly, E. J. McElroy and A. R. Biknevicius, "Posture, gait and the ecological relevance of locomotor costs and energy-saving mechanisms in tetrapods," *Zoology* **110**(4), 271–289 (2007).